Cell

A Role for the Primary Cilium in Notch Signaling and Epidermal Differentiation during Skin Development

Ellen J. Ezratty,[1] Nicole Stokes,[1] Sophia Chai,[1] Alok S. Shah,[1] Scott E. Williams,[1] and Elaine Fuchs[1,*]
[1]Howard Hughes Medical Institute, Laboratory of Mammalian Cell Biology and Development, The Rockefeller University, New York, NY 10065, USA
*Correspondence: fuchslb@rockefeller.edu
DOI 10.1016/j.cell.2011.05.030

SUMMARY

Ciliogenesis precedes lineage-determining signaling in skin development. To understand why, we performed shRNA-mediated knockdown of seven intraflagellar transport proteins (IFTs) and conditional ablation of *Ift-88* and *Kif3a* during embryogenesis. In both cultured keratinocytes and embryonic epidermis, all of these eliminated cilia, and many (not *Kif3a*) caused hyperproliferation. Surprisingly and independent of proliferation, ciliary mutants displayed defects in Notch signaling and commitment of progenitors to differentiate. Notch receptors and Notch-processing enzymes colocalized with cilia in wild-type epidermal cells. Moreover, differentiation defects in ciliary mutants were cell autonomous and rescued by activated Notch (NICD). By contrast, Shh signaling was neither operative nor required for epidermal ciliogenesis, Notch signaling, or differentiation. Rather, Shh signaling defects in ciliary mutants occurred later, arresting hair follicle morphogenesis in the skin. These findings unveil temporally and spatially distinct functions for primary cilia at the nexus of signaling, proliferation, and differentiation.

INTRODUCTION

In response to external cues, embryonic skin cells either stratify, differentiate and generate epidermis, or invaginate and initiate hair follicle (HF) morphogenesis (Fuchs, 2007). The process requires Wnt signals from adjacent epidermal cells and inhibitory BMP signals from underlying mesenchymal condensates, which converge to activate Sonic hedgehog (Shh) in the emerging hair bud. Loss of Shh signaling disrupts this epithelial-mesenchymal crosstalk, impairing HF downgrowth and maturation in the embryo and grossly distorting homeostasis throughout postnatal skin epithelium (Chiang et al., 1999; Gritli-Linde et al., 2007; Oro and Higgins, 2003). Epidermal morphogenesis not only precedes but also occurs independently of Hh signaling (Oro and Higgins, 2003). The transition from basal to suprabasal epidermal fates begins around embryonic day 13.5 (E13.5), when epidermis stratifies as Notch ligands signal through their receptors (Blanpain et al., 2006). This engagement results in enzymatic cleavage of Notch intracellular domain (NICD) and its translocation to the nucleus, where it associates suprabasally with DNA-binding protein RBP-j to activate downstream target genes (Kopan and Ilagan, 2009; Lowell et al., 2000; Moriyama et al., 2008; Okuyama et al., 2004; Wang et al., 2008).

In developing epidermis, Notch signaling triggers a terminal differentiation program that culminates in skin barrier formation (Nguyen et al., 2006). Loss-of-function studies show that NICD-RBP-j activation is essential for the early transition of basal progenitors to committed, suprabasal "spinous" cells, a switch that is typified by downregulation of keratins K5/K14 and induction of K1/K10 and by dramatic downstream architectural changes in cytoskeletal and intercellular adhesion (Blanpain et al., 2006). However, little is known about events residing upstream of Notch-NICD-RBP-j that initiate its activation.

Accumulating evidence suggests that, during development, many mammalian cells, including those of skin, efficiently receive and transmit extracellular signals through a conserved, microtubule (MT)-based sensory organelle called the primary cilium (Bershteyn et al., 2010; Goetz and Anderson, 2010; Santos and Reiter, 2010). The primary cilium emanates from the oldest (mother) of two centrioles, which, with its associated pericentriolar material, constitutes the basal body. Ciliogenesis utilizes an intraflagellar transport (IFT) bidirectional transit system in order to distally elongate the growing microtubule (MT) axoneme (Pedersen and Rosenbaum, 2008). In this system, the MT motor kinesin II facilitates anterograde transport in association with IFT-B, comprising 11 IFTs, including -88, -172, and -74, whereas dynein mediates retrograde transport (toward the basal body) of IFT-A, a complex of approximately six additional IFTs (Goetz and Anderson, 2010). Disruption of either kinesin II or individual IFTs in vertebrates eliminates the primary cilium, resulting in diverse developmental and cell signaling defects known as ciliopathies (Nigg and Raff, 2009).

Much of what is known about primary cilia and signaling comes from embryonic studies linking *Ift* gene mutants to phenotypic defects resembling loss of Shh signaling, whereby ciliary defects act downstream of membrane effectors Patched and Smoothened and upstream of Gli transcription factors

(Huangfu et al., 2003; Goetz and Anderson, 2010). In brain, cilia function in fate specification, proliferation, and overall patterning of neural progenitors (Han and Alvarez-Buylla, 2010), whereas in skin, cilia of dermal papilla (DP) cells have been implicated in Shh-dependent HF morphogenesis (Bershteyn et al., 2010; Gao et al., 2008; Lehman et al., 2009). Cilia are also present in skin epithelia (Elofsson et al.,1984), where they differentially modulate progression to basal cell carcinomas arising from uncontrolled Shh signaling (Wong et al., 2009). Loss of ciliogenesis in postnatal skin epithelium, through conditional targeting of either *Ift88* or *Kif3a*, blocks Shh signaling and disrupts epithelial-mesenchymal crosstalk involved in HF homeostasis (Croyle, et al., 2011).

In skin, Shh signaling is thought to function exclusively in HF morphogenesis and homeostasis, even though postnatal loss of either Shh signaling (Gritli-Linde et al., 2007) or cilia (Croyle et al., 2011) results in elevated proliferation and suppressed differentiation throughout the entire skin epithelium. This is not surprising, as similar postnatal phenotypes occur as a common secondary consequence of alterations in the skin barrier, which can arise from mutations in either HF or epidermal genes (Fuchs et al., 1992; Yi et al., 2006; Blanpain et al., 2006; Luxenburg et al., 2011). That said, in the course of examining changes in MT organization that occur during stratification and differentiation in skin, we became intrigued by the early embryonic appearance of cilia in this tissue at a stage well before HF morphogenesis. This led us to wonder whether primary cilia might be functioning prior to Shh signaling and, if so, what their purpose might be.

In the previously described keratin-Cre *Ift88*-targeted mutant mice, ciliary loss did not occur in embryonic skin epithelium (Croyle et al., 2011), so we turned to developing new animal models and strategies that would enable us to tackle this issue and examine the sequence of events that occur upon ciliary loss. In the present study, we complemented our ability to culture primary epidermal keratinocytes (MKs) in vitro with a powerful new noninvasive lentiviral methodology to efficiently and selectively deliver shRNAs to E9.5 embryos in utero at a stage when skin exists as a single layer of epidermal cells (Beronja et al., 2010). Using a combination of knockdowns and conditional ablations of ciliary genes, we compared 10 different reagents that quantitatively deplete cilia.

Some of these, including *Kif3a* and *Ift88* ablation, also displayed nonciliary defects, such as hypoproliferation and/or alterations in cytoplasmic MTs. However, all ciliary mutants tested showed compromised Notch signaling, as determined by defective NICD-RBPj activation and impaired basal-to-spinous cell fate commitment. Importantly, these early embryonic differentiation defects did not appear to be secondary but, rather, direct and cell-autonomous consequences of ciliary loss. They also preceded and were independent of defects that arise several days later in Shh signaling and HF morphogenesis. Finally, we demonstrate that, as shown previously for components of Shh signaling, Notch components colocalized with ciliary structures at the time of signaling. When cilia were abolished in vivo, activated Notch and Notch reporter activity were diminished concomitantly. Thus, by dissecting the temporal consequences of loss of ciliogenesis in vitro and during embryonic skin development, we have identified two distinct signaling-enhancing functions for cilia operating at different times and lineages to balance growth and differentiation.

RESULTS

Ciliogenesis during Embryonic Epidermal Stratification

To characterize ciliogenesis during skin development, we used whole-mount immunofluorescence (Figure 1 and Figure S1A available online). By E12.5, single-layered skin epithelium displayed primary cilia. Cilia were apically oriented, consistent with the apical position of the centrosome/basal body (Williams et al., 2011) (Figures 1A–1C). They were readily visualized with antibodies against IFT88 and acetylated α-tubulin, a posttranslational modification of stable MTs (Figure 1D). Upon stratification, both basal and suprabasal spinous layers exhibited apically oriented cilia. Whether single layered or stratified, ~60%–75% of cells were ciliated (Figure 1B).

The process of ciliogenesis was recapitulated in MKs cultured from newborn (P0) mice (Figures 1E and 1F). In low (50 μM) calcium media, ~10%–15% of the epidermal monolayer displayed apical primary cilia. After shifting to high (2 mM) calcium to induce stratification and differentiation, ~40%–50% of suprabasal MKs were ciliated.

Ciliogenesis Occurs Independently of Lineage Specification but Requires Cell Polarity

To place ciliogenesis in the context of skin biology, we examined mutant embryos conditionally null for genes that regulate either epithelial polarity or morphogenesis (Figure 1G and Figure S1B). Ciliogenesis was significantly impaired in epidermis lacking essential components of intercellular and cell-substratum adhesion (Raghavan et al., 2000; Vasioukhin et al., 2001). By contrast, cilia were still present in focal adhesion kinase (FAK)-deficient epidermis, which exhibits enhanced adhesion but normal tissue architecture (Schober et al., 2007). Cilia were also intact in embryonic skins lacking Shh, Notch-effector RBP-J, or Wnt-effector β-catenin. Even when epidermis was unable to stratify or form HFs due to loss of stem cell factor p63 (Mills et al., 1999; Yang et al., 1999), cells still polarized and ciliated similar to wild-type (WT). Together, these data place ciliogenesis after epidermal polarization and prior to the signaling and regulatory pathways that specify skin differentiation programs.

Identifying Reagents that Eliminate Cilia and Minimize Nonciliary Defects

To identify appropriate reagents for exploring the functional relevance of epidermal cilia, we infected cultured P0 MKs from *Kif3a* (fl/fl) and (+/fl) pups with a lentivirus-expressing Cre recombinase (LV-Cre). Similar to embryonic skin, uninfected and LV-Cre-infected *Kif3a* (+/fl) MKs formed a stratified epidermal sheet upon 2 mM Ca^{+2} exposure, a process that is associated with cortical redistribution of MTs and reinforcement of intercellular adhesions in terminally differentiating cells (Lechler and Fuchs, 2007) (Figures S2A and S2B). By contrast, LV-Cre-transduced *Kif3a* (fl/fl) cells lacked kinesin II and were defective in ciliogenesis. Although they formed an epidermal sheet in response to Ca^{+2}, E-cadherin labeling was reduced, and perturbations

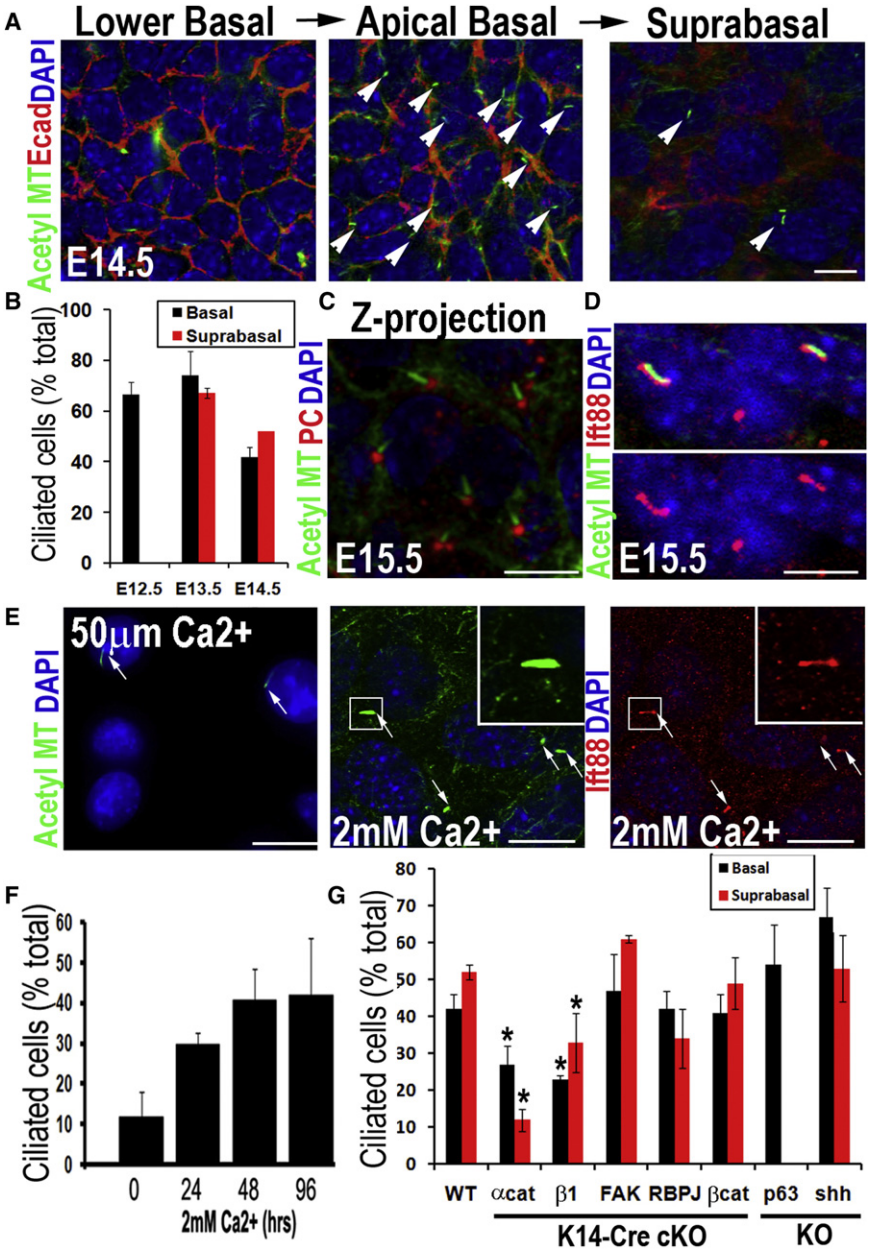

Figure 1. Ciliogenesis in Developing Epidermis Occurs after Cell Polarity and prior to Shh, Notch, and Wnt Signaling

(A and B) Confocal immunofluorescence (IF) of whole-mount epidermis (planar views) was imaged for embryonic days and antibodies (Abs) indicated (color coding according to secondary Abs). Note apically oriented primary cilia in both basal and suprabasal cells. Arrows denote individual primary cilia, visualized by anti-acetylated tubulin. Cell-cell borders denoted by anti-E-cadherin; nuclei marked by DAPI. Histogram represents data from 3–4 embryos/condition, wherein total number of ciliated cells was quantified in basal versus suprabasal layers. n = 300–500 cells/condition. Data are represented as mean ± SEM.

(C) Confocal IF Z-projection of epidermis. Basal body is denoted by pericentrin; primary cilium is visualized by anti-acetylated tubulin.

(D) Confocal IF of cilia colabeled with IFT88 ± acetylated tubulin Abs, as shown.

(E) Differentiation-enhanced ciliogenesis in vitro. MKs before and after Ca^{+2}-induced stratification and differentiation. Arrows denote individual primary cilia visualized by anti-acetylated tubulin or IFT88 Ab staining. Boxed region is magnified.

(F) Histogram represents data from two independent experiments wherein percentage of ciliated cells was quantified at times after shift. n ≥ 500 cells/condition. Data are represented as mean ± SEM.

(G) Ciliogenesis in E15.5 epidermis from mice of the genetically mutant backgrounds indicated. *$p < 0.001$ compared to WT. Histogram provides ciliary quantifications of basal versus suprabasal cells from 3–4 embryos/condition. n = 300–500 cells/condition. Data are represented as mean ± SEM.

Scale bars, 10 μM. See also Figure S1.

were seen in acetylation of cytoplasmic MTs and their cortical reorganization (Figures S2A–S2C).

To distinguish between defects reflecting ciliary loss versus possible nonciliary functions, we searched for IFT proteins that, when depleted by LV-mediated shRNA knockdown (KD), might compromise ciliogenesis without perturbing cytoplasmic MTs. We targeted seven different IFT proteins (Figures 2A–2C). Cultures transduced with scrambled shRNAs behaved similarly to WT and exhibited normal ciliogenesis. In striking contrast, cultures transduced with *Ift* shRNAs all displayed markedly reduced ciliogenesis. Importantly, multiple hairpin shRNAs targeting the same *Ift* showed similar effects. To unequivocally rule out nonspecific or off-target effects, we rescued ciliogenesis with *Ift* expression vectors lacking the targeting sequence (Figure 2D).

Whereas some shRNAs noticeably altered cytoplasmic MT networks (*Ift172-1*) and/or reduced overall levels of acetylated tubulin (*Ift88-1*, *Ift172-1*), IFT74 depletion effectively eliminated cilia without grossly perturbing overall MT architecture and stability (Figure 2A and Figure S2D). Moreover, when MKs depleted of IFT74 were transfected to express mCherry-α-tubulin and were subjected to live cell imaging, their MT dynamics were similar to WT (Figures S2E and S2F).

IFT74, IFT88, and Kinesin II Are Required for Ciliogenesis but Differentially Impact MT Organization and Cell Proliferation In Vivo

To explore the functional relevance of our findings, we cloned *Ift74-1* and scrambled control shRNAs into lentiviral expression vectors for H2B-RFP (to control for infection efficiency in vivo)

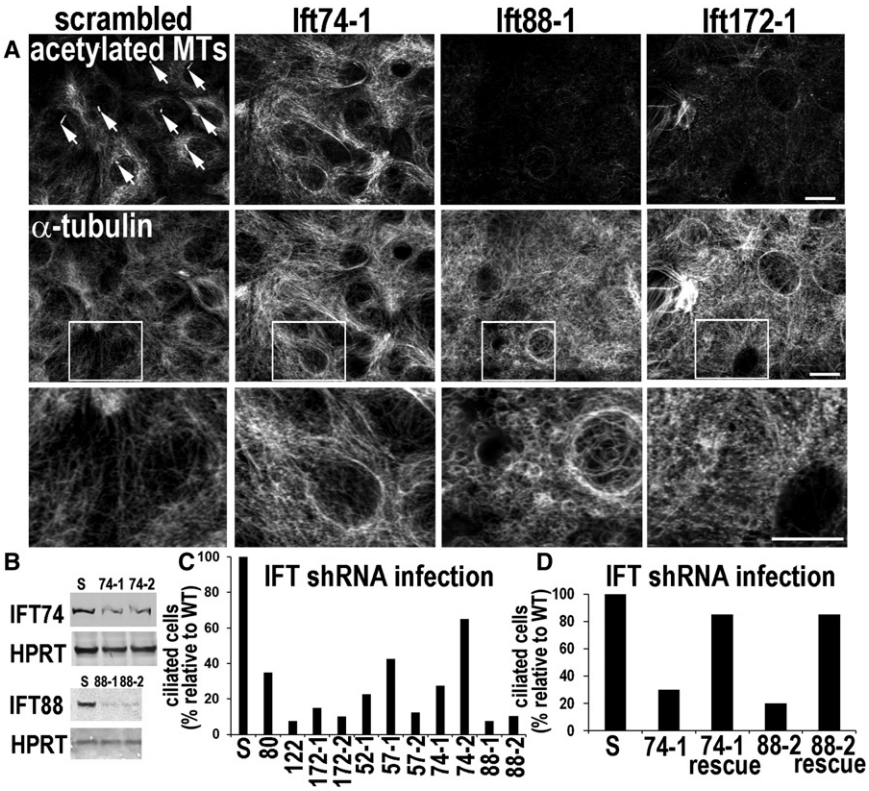

Figure 2. Depletion of IFTs In Vitro Impairs Ciliogenesis but Can Also Elicit Nonciliary Defects in MT Networks

Primary MKs were infected with the lentiviruses indicated, selected for puromycin resistance (viral integration), and then Ca^{+2} shifted 48 hr prior to analyses.

(A) *shRNA*-mediated *Ift* KDs. Depletion of *Ift88* and *Ift172*, but not *Ift74*, reduces levels of acetylated tubulin and inhibits Ca^{+2}-induced MT reorganization. Arrows point to primary cilia present on MKs expressing scrambled shRNAs, but not on cells depleted of IFT74, IFT88, or IFT172. Boxed regions are shown magnified below. Scale bars, 10 μM.

(B) Representative immunoblots of lysates from MKs expressing *Ift*-shRNAs indicated. S, scrambled shRNA; HPRT, loading control.

(C and D) Quantifications of ciliogenesis, showing suppression upon IFT depletion (C) and rescue of ciliogenesis defects upon overexpression of nontargeting Ift74 and Ift88 cDNAs (see Experimental Procedures). Histograms represent data from > 2 independent experiments in which cilia were quantified in shRNA KD cell lines after Ca^{+2} shift. See also Figure S2.

and injected these lentiviruses into amniotic sacs of E9.5 mouse embryos. This noninvasive strategy selectively and efficiently delivers high-titer lentivirus to single-layered embryonic skin epithelium, without perturbing proliferation, differentiation, fate specification, or tissue homeostasis and without infecting underlying dermis (Beronja et al., 2010). Embryos were allowed to develop in utero and were then analyzed between E15.5 and birth. Throughout this time, embryos typically showed transduction of > 85% head skin and ~60%–70% back skin. Because viral DNA stably integrated and embryos grew rapidly, large clonal patches of skin were transduced (Figures 3A and 3B).

Whole-mount fluorescence microscopy and quantitative analyses revealed normal ciliogenesis in both RFP− uninfected and RFP+ scrambled shRNA-transduced clones. By contrast, ciliogenesis was abolished in RFP+ *Ift74* shRNA-transduced regions of E15.5 embryos (Figure 3C). Moreover, *Ift74* KD resulted in loss of cilia not only in basal cells, but also in their suprabasal progeny, readily identifiable by their even brighter H2B-GFP. Given that *Kif3a* conditional targeting has been a widely used tool to explore ciliogenesis, we also conditionally targeted kinesin II with a *K14-Cre* line (Vasioukhin et al., 1999) that efficiently ablated *Kif3a* and ciliogenesis by E15.5 (Figure 3D). Similar to *Kif3a* null epidermal sheets in vitro, *Kif3a-cKO* suprabasal layers in vivo showed reduced acetylated tubulin and aberrations in cortical MT organization (Figure 3E). The embryonic loss of cilia in these two mutants differed from previous studies, wherein cilia still persisted throughout skin development (Croyle et al., 2011).

In comparison to WT, *Kif3a* null embryonic epidermis was thin. Quantifications of S phase cells (BrdU incorporation) and mitotic cells (antihistone H3 immunofluorescence) revealed a clear paucity of proliferation relative to WT (Figures 4A and 4B). This did not seem attributable to enhanced apoptosis, as judged by the absence of activated caspase-3 and apoptotic bodies (Figure S3 and data not shown). However, this hypoproliferative phenotype was in stark contrast to adult *Kif3a* null skin, which was hyperproliferative (Croyle et al., 2011). Phenotypes involving embryonic hypoproliferation followed by postnatal hyperproliferation have previously been observed for gene mutations such as *Rbpj*, which perturb both proliferation and the skin barrier (Blanpain et al., 2006). We return to this issue later.

In contrast to *Kif3a*, epidermal regions transduced with either *Ift74* or *Ift172*, but not scrambled, shRNAs showed hyperproliferation and expansion of K14+ cells (Figures 4C and 4D; data not shown). Moreover, the proliferative difference between *Kif3a* null epidermis and our *Ift* KDs was not attributable to the targeting methodology, as hyperproliferation was also observed in embryos conditionally null for *Ift88* on the background of our *K14-Cre* line (Figures 4E and 4F). To further place the proliferative phenotype within the context of ciliogenesis and distinguish it from secondary defects, we conducted analyses in vitro, wherein the microenvironment was uniform and well defined. *Kif3a* null MKs were hypoproliferative, whereas MKs expressing most *Ift* shRNAs showed signs of faster growth. These proliferative differences were substantiated by staining for Ki67 (elevated in S and M phase cells) and were rescued by *Ift74* and *Ift88* expression vectors (Figures 4G–4J).

Finally, the relatively low number of ciliated basal cells in vitro (Figure 1F) suggested that ciliogenesis might inversely correlate with proliferation, which, in WT, is higher in cultured MKs than in

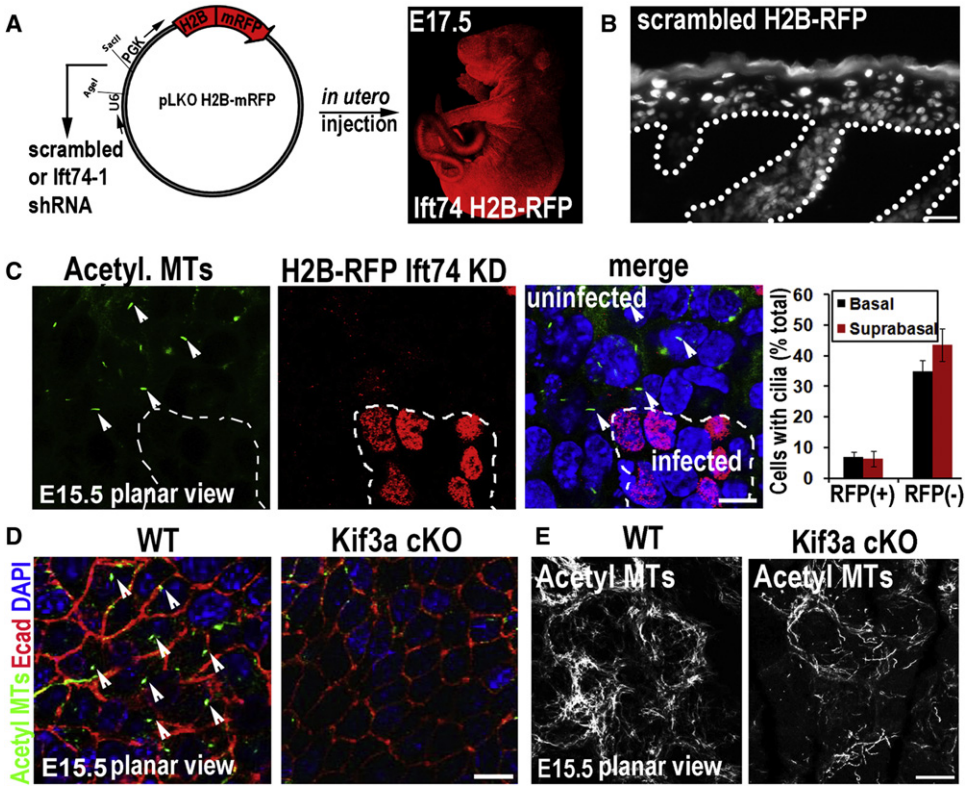

Figure 3. In Utero Knockdown of *Ift74* or Conditional Knockout of *Kif3a* Impairs Ciliogenesis in Developing Epidermis

(A) Modified vector used to produce high-titer lentivirus and H2B-RFP/*Ift74-1* shRNA-transduced embryo.

(B) Immunofluorescence shows that viral infection at E9.5 was restricted to epidermis, propagating H2B-RFP/scrambled shRNA expression to all progeny of infected cells.

(C) Cilia (arrows) are eliminated in *Ift74-1* shRNA-transduced epidermal cells (RFP+), but not neighboring uninfected cells. Histogram represents mean data from 2–3 embryos in which cilia were quantified in RFP+ versus RFP− basal and suprabasal cells from E15.5 epidermis. n = 200–600 cells/condition. Bars are SEM.

(D) *Kif3a* cKO inhibits ciliogenesis in comparison to WT. Arrows denote cilia.

(E) Loss of kinesin-II reduces acetylated MTs in vivo (as in vitro). Scale bars, 10 μM.

embryonic epidermis. Immunofluorescence for acetylated tubulin and Ki67 revealed that, whether in vivo or in vitro, most actively cycling epidermal cells did not display a cilium (Figure 4H). These findings are in good agreement with the view that cilia are disassembled prior to mitosis (Pan and Snell, 2007). Taken together with the significant hyperproliferation of IFT74-deficient cells displaying minimal nonciliary alterations, we conclude that hyperproliferation is a direct consequence of ciliary loss.

Ciliary Loss Results in Defective Epidermal Differentiation and Notch Signaling Independent of Defects in Proliferation or HF Morphogenesis

The enhanced proliferation and expansion of basal-like cells in our IFT74-deficient embryos suggested that ciliary loss might directly affect epidermal differentiation independently of the anticipated secondary consequences of compromising Shh signaling and HF morphogenesis. To test this hypothesis, we first examined the effects of *Ift74-1* KD on Ca^{+2}-induced terminal differentiation in vitro. Only MKs transduced with scrambled shRNA, and not *Ift74-1* shRNA, generated differentiating K1/K10-expressing spinous cells upon a Ca^{+2} shift (Figure 5A). Similar results were obtained with the chemical chloral hydrate, which selectively cleaves the cilium from its basal body (Chakrabarti et al., 1998; Kennedy and Brittingham, 1968). At 2 mM chloral hydrate, MKs showed no overt cytoplasmic MT defects, but both ciliogenesis and Ca^{+2}-induced K10 expression were abrogated (Figure S4 and Figures 5B and 5C).

K10 expression and basal-to-spinous fate transition require Notch signaling (Blanpain et al., 2006; Nguyen et al., 2006). To determine whether this pathway is influenced by ciliary loss, we cloned control and *Ift* shRNAs into a lentiviral H2B-RFP vector containing a Notch GFP reporter gene (Williams et al., 2011; Figure S4A). In WT MKs or MKs expressing scrambled shRNA, GFP was strongly elevated upon Ca^{+2} shift. By contrast, cells expressing shRNAs for *Ift74*, *Ift172*, or *Ift88*-shRNAs all displayed significantly reduced Notch reporter activity (Figures 5D and 5F). Moreover, cultured MKs from P0 Notch reporter GFP mice only exhibited strong K10 and GFP Notch reporter activation when shifted to $Ca2^{+}$ in the absence and not presence of chloral hydrate (Figures 5E and 5G).

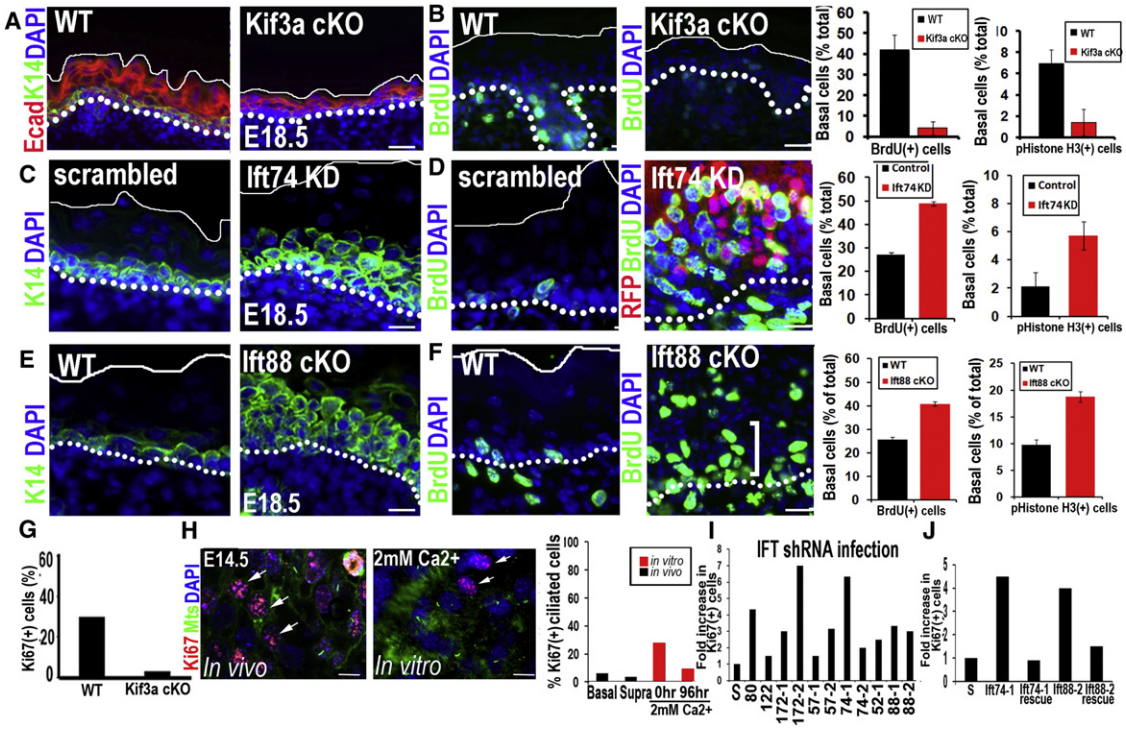

Figure 4. Depletion of IFTs versus Kinesin II Causes Opposing Defects on Cell Proliferation

(A) *Kif3a* cKO epidermis is thin compared to WT littermate controls.

(B) Kinesin II-deficient epidermis is hypoproliferative. Quantifications of BrdU incorporation and phospho-H3+ cells in *Kif3a* WT versus cKO epidermis. Data are from two embryos.

(C–F) *Ift74* KD and *Ift88* cKO results in expansion of K14-expressing layers and hyperproliferation compared to scrambled or WT control. Abs/epifluors are color coded. Quantifications of BrdU and phospho-H3 in WT and *Ift74*-shRNA-expressing cells. Histogram represents data from two embryos in which BrdU+ basal cells were quantified. n = 700–1000 cells/condition.

(G) Quantification of cell proliferation in LV-Cre transduced Kif3a (fl/fl) and (+/fl) MKs.

(H) Inverse correlation between a cilium and the S/M phase of the epidermal cell cycle. Histogram represents data from ≥ 2 experiments in which percent of Ki67+ S/M phase ciliated cells were quantified in E14.5 basal and suprabasal epidermal cells in vivo or in MKs cultured 96 hr in medium containing Ca^{+2} levels indicated. Primary cilia are rarely observed in Ki67+ cells (arrows).

(I) Quantification of cell proliferation in various IFT KD cell lines.

(J) Rescue of cell hyperproliferation upon expression of nontargeting IFT74 and IFT88 (see Experimental Procedures). Histograms in (G)–(H) represent data from ≥ 2 experiments in which percent of Ki67+ S/M phase ciliated cells were quantified.

All data are represented as mean, and error bars are ± SEM. Scale bars: (A), (C), and (E), 40 μM; (B), (D), and (F), 20 μM; (H) 10 μM. See also Figure S3.

To address whether Notch signaling is perturbed in vivo when ciliogenesis is defective, we conducted in utero infections with our Notch reporter/H2B-RFP lentiviruses expressing either scrambled or *Ift74* shRNA (Figure 6A). As expected, many suprabasal RFP+ cells in control embryos induced the Notch reporter (GFP). In contrast, reporter activity was markedly diminished in *Ift74*-transduced embryos.

Consistent with defective Notch signaling, *Ift74* shRNA clones showed reduced K10 (Figure 6B). Importantly, K10 was still expressed in adjacent uninfected skin patches, suggesting that the defects were cell autonomous and not due to general skin perturbations. Furthermore, these defects did not seem to arise from off-target effects of *Ift74-1* KD, as even though *K14-Cre*-mediated *Ift88* cKO embryonic epidermis showed a greater delay in ciliary loss than *Ift74-1* KD, it still showed reduced K10 and signs of defective Notch/NICD signaling (Figures S5A–S5C). *Kif3a* cKO embryos also showed diminished K10 (Figure 6B). Because *Kif3a* mutant embryos were hypoproliferative (Figure 4), the basal-to-spinous cell fate defect in Ift74 KD skin did not seem to be merely a secondary consequence of hyperproliferation.

Importantly, basal-to-spinous cell defects could be partially rescued by transgenic expression of NICD, suggesting that defects in Notch signaling were directly linked to loss of IFT74 and cilia (Figure 6C). Finally, irrespective of whether kinesin-II, IFT74, or IFT88 was deficient, apical localization of LGN, required for asymmetric cell division and upstream Notch signaling (Williams et al., 2011), was unaffected, as was overall orientation of mitotic spindles (Figures S5D–S5F; data not shown; see also Croyle et al., 2011).

We also observed diminished Hes1 (Figures 6D and 6E). Though this Notch target gene can also be induced by other pathways and is not essential for basal to spinous cell differentiation (Moriyama et al., 2008), its reduced presence suggested

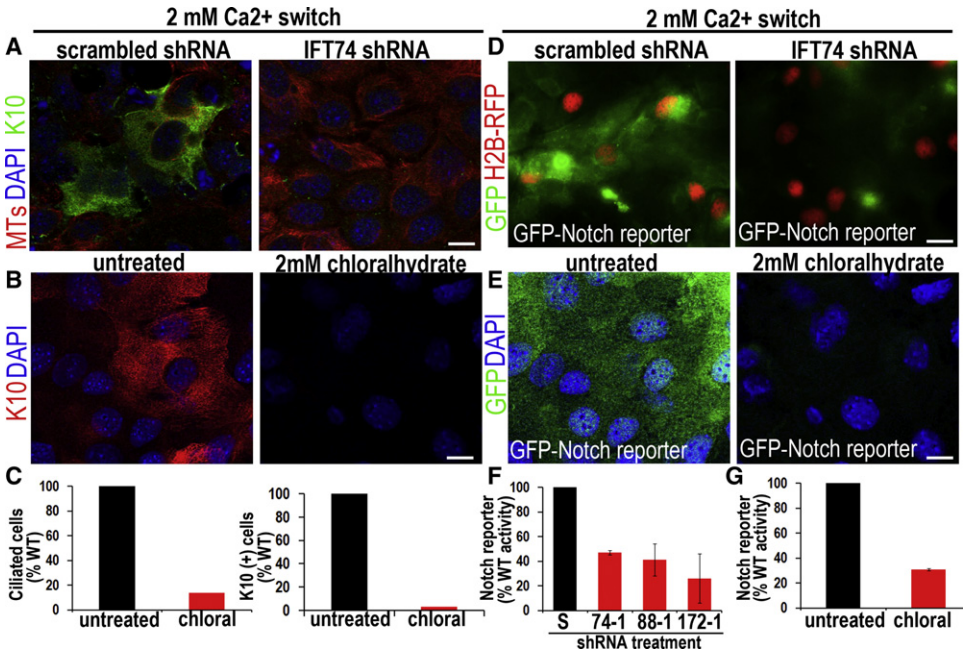

Figure 5. Loss of Primary Cilia Directly Inhibits MK Differentiation and Notch Reporter Activity

(A) In vitro, Ca^{+2} induces K10 in MKs expressing scrambled control, but not *Ift74* shRNAs.

(B) Chloral hydrate treatment blocks both ciliogenesis and K10 induction under conditions in which cytoplasmic MTs are unaffected (see also Figure S4).

(C) Histograms represent data from two independent experiments in which ciliated and K10-expressing cells were quantified and compared to untreated control cells. n $\geq$ 200 cells/condition.

(D–G) P0 MKs from a transgenic Notch reporter mouse also show Ca^{+2}-induced Notch activity, diminished by chloral hydrate or KD of *Ift74*, *Ift88*, or *Ift172*. Histogram in (F and G) represents data from > 2 independent experiments in which GFP IF was measured in the shRNA-expressing or chloral hydrate-treated cells and compared to scrambled controls. Histogram represents averaged data from two independent experiments in which > 200 cells/condition were analyzed. Error bars are ± SEM. Scale bars, 10 μM. See also Figure S4.

that Notch signaling was defective in *Ift74 KD* or *Kif3a* cKO embryonic epidermis. Later-stage terminal differentiation-specific proteins such as filaggrin and involucrin were also diminished (shown). Consistent with these epidermal defects, E17.5 mutant embryos showed reduced capacity for excluding blue dye relative to controls (Figure 6F). There did not seem to be a developmental delay, as embryos were similar in size to control animals. However, they died shortly after birth, similar to loss-of-function mutants in RBP-j.

Loss of Ciliogenesis Affects Shh Signaling in HFs Later in Embryogenesis

Given the well-established role of ciliogenesis on Shh signaling and the importance of Shh signaling in crosstalk between DP and HF epithelium, we were intrigued by studies showing apparent conversion of HF to epidermis when cilia are ablated in postnatal skin epithelium, but not in DP (Croyle et al., 2011). To delve deeper into these differences and place them in the context of our findings, we first tested whether loss of Shh signaling, anticipated from ciliary loss, might indirectly affect Notch signaling in epidermis. Analysis of *Shh* null epidermis at E15–E17 showed that Notch signaling components were expressed and properly localized in the stratified, differentiating spinous layers (Figure S6A). Moreover, during WT embryogenesis, Gli1 and Gli2 were only detected in developing HFs and not stratifying epidermis (Figures S6B). These data did not favor the view that the early embryonic defects in Notch signaling and epidermal differentiation arose secondarily from altered Shh signaling.

Ablation of cilia did result in altered Shh signaling, as predicted from its postnatal consequences in basal cell carcinoma-like and HF phenotypes (Wong et al., 2009; Croyle et al., 2011). Thus, HF morphogenesis was arrested and Gli2 reduced in our ciliary-deficient embryos, consistent with a loss of Shh signaling in skin (Figures S6C–S6E). Importantly, this was the case irrespective of whether epidermis was hyperproliferative or hypoproliferative, as revealed by the similar consequences from kinesin II loss (Figures S6C–S6D). Together, these data suggest that cilia play dual roles during skin development: an early Shh-independent role in regulating Notch signaling and balancing proliferation and differentiation in the epidermis and a late, Shh-dependent role during HF morphogenesis.

Interestingly, similar to prior reports (Goetz and Anderson, 2010), loss of ciliogenesis in limb resulted in polydactyly, a hallmark of ectopic Shh signaling (Figure S6F). Although this gain of Shh signaling defect is beyond the scope of our study, the differences in how these two Shh-sensitive tissues respond to ciliary loss provided further evidence that ciliary function(s) in epithelial tissues are context dependent and complex.

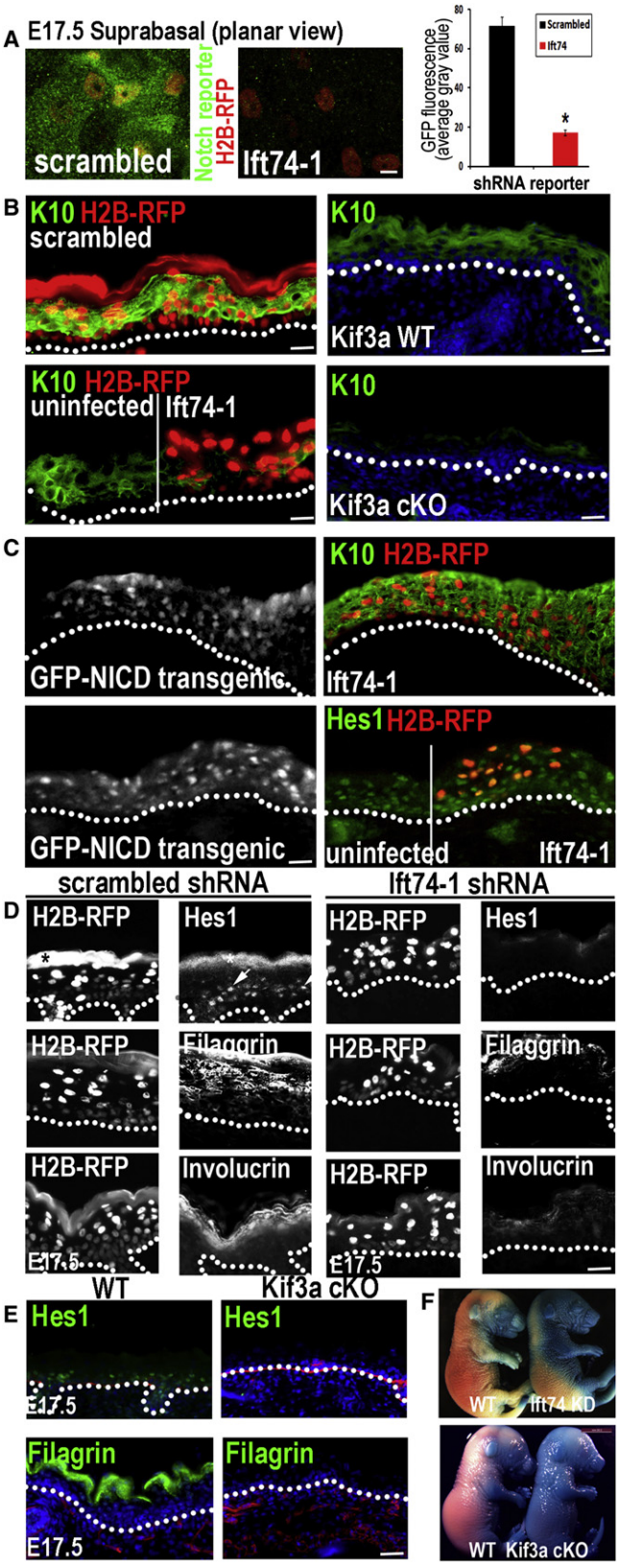

Figure 6. Elimination of Primary Cilia In Vivo Diminishes Notch Signaling and Inhibits Basal to Spinous Cell Fate Commitment in Developing Epidermis

(A) Confocal images showing that Notch reporter activity (GFP) is induced suprabasally in E17.5 spinous epidermal cells expressing scrambled, but not *Ift74*, shRNAs. Transduced cells are H2B-RFP+. Quantifications reveal 5× less GFP reporter expression in Ift74-deficient versus control cells. Histogram represents averaged data from 2–3 embryos in which > 200 RFP+ cells were analyzed. *p < .001 by students t test. Error bars are ± SEM. Scale bar, 10 μM.

(B) H2B-RFP(+) *Ift74*-shRNA transduced areas show reduced K10 compared to adjacent uninfected or scrambled shRNA-transduced epidermis. *Kif3a* cKO epidermis similarly shows diminished K10 in comparison to WT.

(C) Transgenic expression of NICD-GFP rescues *Ift74* shRNA-induced defects in K10 and Hes1 expression.

(D and E) Repression of differentiation markers Hes1, filaggrin, and involucrin correlates with loss of cilia rather than proliferative status. Transduced areas of hyperproliferative *Ift74*-shRNA-knockdown epidermis. (D) (H2B-RFP+) show reduced differentiation compared to scrambled controls. *denotes background fluorescence; arrows note nuclear Hes1. Hypoproliferative *Kif3a* cKO epidermis (E) shows similar diminished differentiation.

(F) Failure to exclude blue dye indicates defective skin barrier formation in *Ift74*-shRNA-transduced and *Kif3a* cKO E17.5 embryos.

(B–E) Scale bars, 45 μM except for Kif3a data, in which scale bar, 100 μM. See also Figure S5 and Figure S6.

Notch Signaling Occurs Preferentially in Ciliated Cells In Vivo and Correlates with Colocalization of Pathway Components to Ciliary Structures

Given the intriguing correlation between ciliogenesis and Notch signaling and our observation that ciliogenesis occurs prior to and independently of both canonical Notch and Shh signaling in skin embryogenesis (see Figure 1G), we wondered whether components of the pathway localize to either the basal body or primary cilium in a fashion analogous to what has been observed for Shh signaling (Goetz and Anderson, 2010). To address this question, we first identified antibodies that, by immunoblot, were specific to endogenous full-length Notch3 receptor, NICD3, and Presenilin-2, the catalytic subunit of γ-secretase that cleaves Notch receptor to generate NICD (Bray, 2006; Tien et al., 2009) (Figure S7A).

In vivo, Presenilin-2 was prominent in spinous layers, where Notch activation is known to occur (Figure S7B). Whole-mount immunofluorescence revealed a honeycomb pattern of Presenilin-2 delineating membranous intercellular borders between spinous cells (Figure 7A). Within a subset of spinous layer cells, intense labeling was also detected at the basal body, comarked by acetylated tubulin. In contrast to Presenilin-2, antibodies against full-length Notch3 were brightest along the length of primary cilia, suggesting that this receptor might be enriched in the ciliary membrane (Figure 7B). This was best visualized in vivo in whole-mount planar views of skin colabeled for acetylated tubulin and Notch 3 (Figure 7B). This immunolocalization appeared to be specific for cilia only in suprabasal cells, where Notch signaling is active. Moreover, such colocalizations were not observed with antibodies against E-cadherin (Figure 7C) or Z0-1 (data not shown) and hence did not seem attributable to a general enrichment of plasma membrane at the ciliary surface. Quantifications of our immunolocalization studies are provided in Figure 7D. Similar colocalizations were observed in vitro, where upon Ca^{+2} shift to induce Notch signaling and spinous fate

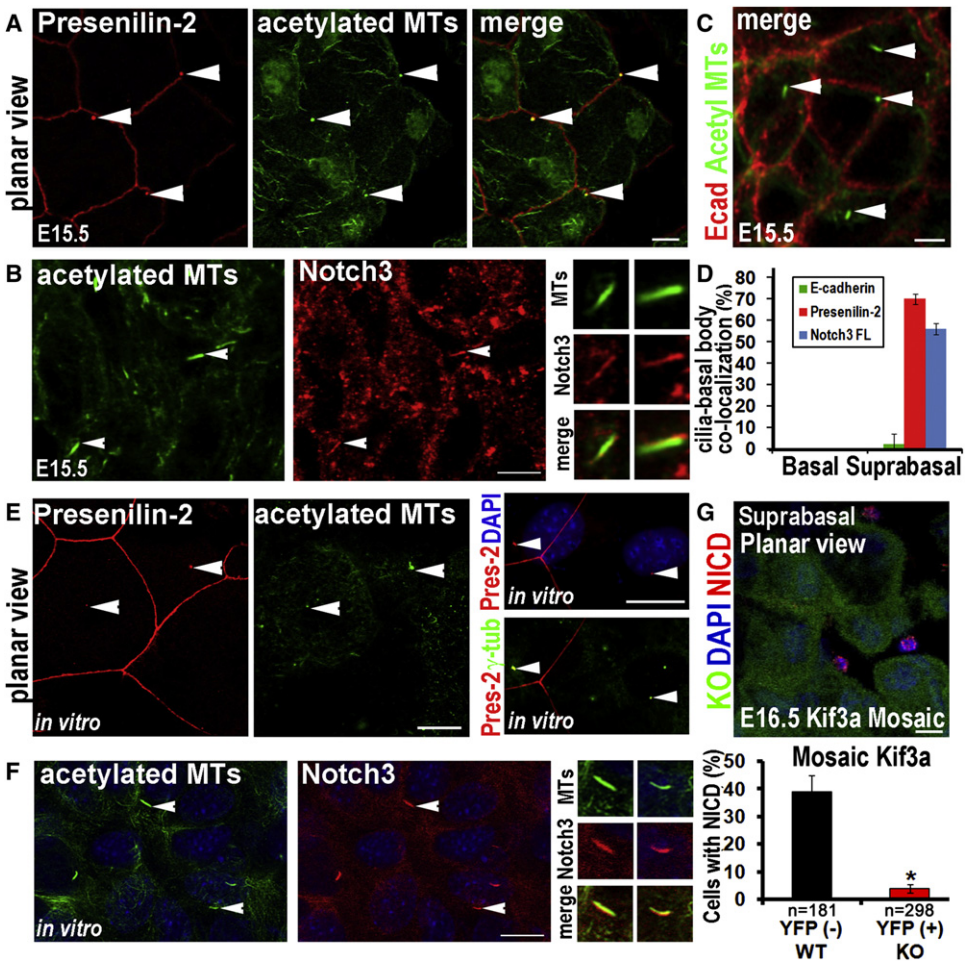

Figure 7. Notch Signaling Components Are Enriched at Primary Cilia in Suprabasal Epidermal Cells

(A) Whole-mount immunolocalization of Presenilin-2 (red) at basal body/ciliary structures (green) in suprabasal cells of developing E15.5 epidermis.

(B) Whole mount of suprabasal E15.5 epidermis shows enriched Notch 3 receptor immunolocalization at a subset of acetylated tubulin+ cilia (arrows), shown magnified in right panels. Neither Presenilin-2 nor Notch 3 receptor was detected in the basal bodies/cilia in basal layer confocal planes.

(C) Whole mount of suprabasal E15.5 epidermis shows lack of E-cadherin labeling (red) at cilia (green; arrows).

(D) Quantification of percent of cilia with E-cadherin, Presenilin-2 or Notch 3 colocalization in basal and suprabasal confocal planes of E15.5 epidermis. $n \geq 100$ cells/condition. Data are represented as mean ± SEM.

(E) In vitro localization of Presenilin-2 at basal body/ciliary structures and in vitro colocalization of Presenilin-2 and the basal body/centrosome marker γ-tubulin.

(F) In vitro localization of Notch 3 at cilia in differentiating MKs. Arrows point to individual cilia shown magnified in the panels at right.

(G) E16.5 mosaic skin from Kif3a cKO epidermis. Note that WT cells (YFP−) show NICD3 nuclear accumulation (red), and adjacent Kif3a null cells (YFP+) lack nuclear NICD3. Quantification of NICD(+) Kif3a cKO versus WT cells, wherein 200–300 cells from 2–3 embryos were quantified/per condition. Data are represented as mean ± SEM. Scale bars, 10 μM.

See also Figure S7.

commitment, Presenilin-2 localized to the ciliary base (Figure 7E). The identity of this structure was further confirmed by colocalization with acetylated tubulin and γ-tubulin, which mark the basal body. Notch 3 also was enriched in the ciliary membrane upon Ca^{+2} shift (Figure 7F).

Finally, if these immunolocalization patterns are functionally relevant, then we would expect to see processed Notch 3, i.e., NICD3, specifically in the nuclei of ciliated suprabasal cells. Moreover, this localization should be compromised when ciliogenesis is genetically abolished. To test this hypothesis, we performed whole-mount anti-NICD3 immunofluorescence on E16.5 *K14-Cre X Kif3a fl/fl X Rosa YFP lox-stop-lox* mosaic embryos, where cKO cells that express active Cre recombinase are YFP+ (Figure 7G). Suprabasal cells within Kif3a mutant (YFP+) patches were uniformly negative for nuclear NICD3. By contrast, ~40% of YFP− suprabasal cells showed nuclear NICD3, reflective of Notch processing/activation. Moreover, because NICD3+YFP− cells could be found adjacent to NICD3−YFP+ ones, these data argue against possible secondary effects caused by gross tissue disruptions and suggest that Notch processing is regulated via a cell-autonomous mechanism.

DISCUSSION

In this study, we unearthed distinct and major roles for primary cilia during embryonic skin development. In epidermis, cilia presence stimulated canonical Notch signaling, thereby balancing proliferation and differentiation. Several days later, cilia functioned in the developing HFs, where they enhanced Shh signaling and promoted morphogenesis.

Ciliogenesis and Cell Polarity

We were intrigued by our findings that mutant embryos null for *p63* displayed cilia, whereas those with disruptions in either epidermal-substratum adhesion (β1-integrin) or adherens junctions (α-catenin) displayed fewer cilia than normal. Because cell polarity is important for proper ciliogenesis (Gerdes et al., 2009), it is tempting to speculate that faulty ciliogenesis may, at least partially, account for the phenotypic abnormalities in *β1* and *α-catenin* mutant embryos. It is less clear whether the converse is true, i.e., whether primary cilia participate in establishing apical-basolateral polarity. Many features of epidermal basal cell polarity seemed intact without cilia, including cell-substratum and intercellular adhesion and mitotic spindle orientation. Moreover, though loss of Kif17, Kif3a, and Ift88 all compromise epithelial polarity, this could be through their non-ciliary rather than ciliary roles (Fan et al., 2004; Lin et al., 2003; Taulman et al., 2001; Jaulin and Kreitzer, 2010). When our findings on Kif3a and Ift88 are coupled with increasing evidence in other systems for secondary and/or additional functions for ciliary proteins (Haraguchi et al., 2006; Baldari and Rosenbaum, 2010; Finetti et al., 2009), these issues merit caution when distinguishing cause from effect.

Additional insight into how β1-integrin and α-catenin loss might impact ciliogenesis emerges from the intriguing discovery that, in HF DP, the actin regulatory protein "Missing-in-Metastasis" is required for ciliogenesis through a mechanism involving Src-kinase activation and Cortactin regulation (Bershteyn et al., 2010). Because F-actin is required for docking the basal body during ciliogenesis (Pan and Snell, 2007) and both α-catenin and β1-integrin interface adhesive junctions with actin dynamics, actin alterations could contribute to the defective ciliogenesis that we observed. Moreover, it is notable that both Src and Cortactin activity can be differentially modulated via β1-integrin-mediated signaling.

Although the cilium is not required for entry into S phase, growth factor signals can trigger its disassembly from the mother centriole prior to mitosis (Pan and Snell, 2007; Schneider et al., 2005; Seeley and Nachury, 2010). Growth factor exposure to retinal epithelial cells elevates focal adhesion-associated protein HEF1 and recruits it to the premitotic basal body, where it triggers MT deacetylation and ciliary disassembly (Pugacheva et al., 2007). Consistent with the cell cycle-dependent depolymerization of cilia that occurs in retinal epithelial cells in vitro, we rarely observed cilia in S or M phase embryonic basal cells in vivo. Moreover, in embryonic basal cells, we detect HEF1 at sites of integrin cell-substratum adhesion (E.J.E. and E.F., unpublished data). Although outside the scope of the present study, it would be interesting to investigate whether the β1-dependent reduction in ciliogenesis might reflect mislocalization of HEF1 and/or secondary consequences of defects in actin dynamics and cell polarity.

Ciliogenesis, Proliferation, and Differentiation

Though waves of ciliary disassembly may drive the cell cycle, permanent loss of ciliogenesis is often associated with constitutive proliferation (Seeley and Nachury, 2010). This appeared to be the case for adult skin epithelium targeted for *Kif3a* and *Ift88* (Croyle et al., 2011), although interpretation is complicated by the possibility that the gross defects in HFs could have affected the skin barrier, thereby perturbing epidermal homeostasis. By targeting ciliary ablation in embryonic epidermis and cultured MKs, we eliminated these caveats. Under these conditions, loss of ciliary components resulted in epidermal hyperproliferation at a time preceding HF perturbations and when postnatal consequences from compromising the skin barrier were not a threat.

Because epidermal hyperproliferation is often countered by suppressed differentiation, we were not surprised initially by diminished signs of terminal differentiation in IFT74-deficient epidermis. It also did not seem particularly remarkable that Notch signaling was perturbed because this pathway is a barometer of the transition from epidermal proliferation to differentiation (Blanpain et al., 2006; Nguyen et al., 2006). However, the defects in Notch signaling and basal-to-spinous fate commitment were still present in hypoproliferative *Kif3a* mutant embryos lacking cilia, thereby uncoupling the suppressed differentiation from proliferation status, but not from ciliary loss.

In considering other possibilities for how defective ciliogenesis might lead to these differentiation defects, we next investigated whether asymmetric cell divisions might be compromised by ciliary ablation. However, spindle orientation appeared to be unaffected in our mutant embryos, consistent with that reported for adult epidermis lacking cilia (Croyle et al., 2011). This contrasted with prior speculation for intestinal stem cells (Satir et al., 2010) and kidney (Jonassen et al., 2008) and prompted us to continue our pursuit of alternative explanations.

Dissecting Shh and Notch Signaling Defects

By analyzing ciliogenesis during early embryogenesis, we discovered that ciliary loss can impact Notch signaling and directly compromise epidermal differentiation and skin barrier function. Ciliogenesis, stratification, and Notch signaling are considerably upstream from Shh signaling and HF morphogenesis in skin development. Indeed, Hes1, Notch3 receptor, and the enzymatically cleaved NICD all appeared to be properly localized in *Shh* null embryonic epidermis (Figure S6). Furthermore, epidermal stratification and differentiation also occurred in skins of mice conditionally targeted for *Smoothened* and hence deficient in all types of Hh signaling (Gritli-Linde, et al., 2007). Thus, loss of Shh signaling was not sufficient to account for the early epidermal defects in our ciliary mutants.

Might aberrations in epidermal differentiation stem from ciliary-mediated, ligand-independent defects in the Hh pathway? Our studies suggest not, as temporally, epidermal differentiation precedes Gli1 and Gli2 expression in HFs by several days. Furthermore, although the Gli3 repressor that silences Hh target genes is diminished when cilia are lost in the

limb (Goetz and Anderson, 2010), Shh signaling and target gene expression appear to be repressed rather than activated in epidermis (Croyle et al., 2011). Finally, Notch signaling defects have not been linked with either *Shh* null or *Shh* overactivation phenotypes in skin.

Rather, our results favor the notion that cilia could function directly in fine-tuning the Notch-regulated balance between proliferation and differentiation in developing skin. The enrichment of Notch and Presenilin-2 in suprabasal ciliary structures supports this view, as does the diminished suprabasal NICD3, Hes1, and Notch activity in mutants in which ciliogenesis is compromised. Our data best fit a model whereby the cilium enhances Notch processing to generate NICD, which with RBP-j, then activates Notch target genes to induce basal-to-spinous fate transition. This model parallels the mechanism for how cilia are thought to transmit a Shh signal. Future experiments are now needed to determine whether Notch signaling components simply fail to be excluded from the cilium or, if they are selectively targeted, which of emerging ciliary trafficking mechanisms is involved.

A few final points are worthy of discussion. In lung epithelium, Notch acts upstream of ciliogenesis (Morimoto et al., 2010), whereas embryonic epidermis displays cilia well before canonical Notch signaling occurs. Moreover, basal and spinous layers exhibit differential ciliary location and signaling of the Notch receptor. To some extent, this may just be a matter of differential expression. However, the link between Notch signaling and cilia is likely to be cell type and context dependent. Although the molecular rationale remains a mystery, it may be relevant that asymmetric divisions can result in differential inheritance of mother centriolar proteins, which temporally regulate ciliogenesis (Wang et al., 2008; Yamashita et al., 2007). If this happens in skin, asymmetric cell divisions could result in functionally distinct basal bodies/cilia at the basal-to-spinous layer interface. Because Notch signaling was recently linked to asymmetric cell divisions in embryonic epidermis (Williams et al., 2011), this could also explain the specific reliance of Notch signaling on ciliogenesis in some, but not all, contexts. Alternatively, Notch signaling might be spatially regulated through ciliary signaling or asymmetric cell divisions involving mutually exclusive mechanisms. Our findings now pave the way for future investigation in this arena.

EXPERIMENTAL PROCEDURES

Generation of Mice

Kif3a fl/fl mice were provided by L. Goldstein (HHMI, UCSD) (Marszalek et al., 1999) and crossed to *K14-Cre* (Vasioukhin et al., 1999) and/or *Rosa26 lox/stop/lox* (Soriano, 1999) mice. Transgenic *Notch reporter* mice (Mizutani et al., 2007) were obtained from Jackson laboratories and outbred to a CD1 background, where they were maintained as homozygotes. See Extended Experimental Procedures for other mice.

Cell Culture, In Vitro Lentiviral Infection, and Immunofluorescence

MKs were isolated and cultured from dispase-treated skins of WT CD-1, *Kif3a fl/fl* or *+/fl*, and transgenic *Notch reporter* mice. After replating at 1×10^5 cells/6-well, cells were infected with $> 10^9$ cfu lentivirus (*NLS-Cre*, *scrambled* control, or *Ift* shRNAs) in the presence of 100 μl/ml polybrene. At 24–48 hr after infection, cells were selected with 1–2 μg/ml puromycin, grown to confluency on fibronectin-coated coverslips, and then shifted to 2 mM Ca^{2+}-containing media (Beronja et al., 2010). At 48 hr later, coverslips were fixed in either −20°C methanol (to visualize the MT cytoskeleton) or 4% formaldehyde before processing for immunofluorescence. For chloral hydrate (Sigma) experiments, *Notch reporter* MKs were plated on fibronectin-coated coverslips and grown to confluency before shifting to media containing 2 mM Ca^{+2} and 2 mM chloral hydrate for 48 hr.

shRNA Constructs and In Utero Lentiviral Injections

Lentiviral shRNAs (TRC-1 Library, Sigma) were cloned into a modified pLKO backbone containing *Notch reporter GFP* and/or *H2B-mRFP* transgenes. The lentiviral *Notch reporter* was generated by cloning a KpnI-XbaI fragment containing four CBF1-binding elements, SV40 minimal promoter, and EGFP from Addgene clone 177051 (Duncan et al., 2005) into pLKO *scramble* or *Ift74 H2B-RFP-1*. See Extended Experimental Procedures for shRNA hairpin sequences. Generation of high-titer lentivirus and in utero injections of E9.5 embryos were as described (Beronja et al., 2010).

SUPPLEMENTAL INFORMATION

Supplemental Information includes Extended Experimental Procedures and seven figures and can be found with this article online at doi:10.1016/j.cell.2011.05.030.

ACKNOWLEDGMENTS

We thank L. Goldstein (UCSD) for Kif3 fl/fl mice and Q. Zhang (University of Iowa) for Ift88 fl/fl mice; D. Oristan and L. Polak for their expertise and assistance in the mouse facility; A. North and the RU Bioimaging Resource Center for assistance with image acquisition; and M. Schober, D. Devenport, C. Luxenburg, M. Kadaja, and other Fuchs laboratory members for helpful discussions and critical reading of the manuscript. E.J.E. is a Jane Coffin Childs postdoctoral fellow, A.S.S. is a Marie Josee and Henry Kravis postdoctoral fellow, S.E.W. is an American Cancer Society postdoctoral fellow, and E.F. is an investigator in the Howard Hughes Medical Institute. This work was supported by a grant from the National Institutes of Health.

Received: September 3, 2010
Revised: March 28, 2011
Accepted: May 23, 2011
Published: June 23, 2011

REFERENCES

Baldari, C.T., and Rosenbaum, J. (2010). Intraflagellar transport: it's not just for cilia anymore. Curr. Opin. Cell Biol. *22*, 75–80.

Beronja, S., Livshits, G., Williams, S., and Fuchs, E. (2010). Rapid functional dissection of genetic networks via tissue-specific transduction and RNAi in mouse embryos. Nat. Med. *16*, 821–827.

Bershteyn, M., Atwood, S.X., Woo, W.M., Li, M., and Oro, A.E. (2010). MIM and cortactin antagonism regulates ciliogenesis and hedgehog signaling. Dev. Cell *19*, 270–283.

Blanpain, C., Lowry, W.E., Pasolli, H.A., and Fuchs, E. (2006). Canonical notch signaling functions as a commitment switch in the epidermal lineage. Genes Dev. *20*, 3022–3035.

Bray, S.J. (2006). Notch signalling: a simple pathway becomes complex. Nat. Rev. Mol. Cell Biol. *7*, 678–689.

Chakrabarti, A., Schatten, H., Mitchell, K.D., Crosser, M., and Taylor, M. (1998). Chloral hydrate alters the organization of the ciliary basal apparatus and cell organelles in sea urchin embryos. Cell Tissue Res. *293*, 453–462.

Chiang, C., Swan, R.Z., Grachtchouk, M., Bolinger, M., Litingtung, Y., Robertson, E.K., Cooper, M.K., Gaffield, W., Westphal, H., Beachy, P.A., and Dlugosz, A.A. (1999). Essential role for Sonic hedgehog during hair follicle morphogenesis. Dev. Biol. *205*, 1–9.

Croyle, M.J., Lehman, J.M., O'Connor, A.K., Wong, S.Y., Malarkey, E.B., Iribarne, D., Dowdle, W.E., Schoeb, T.R., Verney, Z.M., Athar, M., et al.

(2011). Role of epidermal primary cilia in the homeostasis of skin and hair follicles. Development *138*, 1675–1685.

Duncan, A.W., Rattis, F.M., DiMascio, L.N., Congdon, K.L., Pazianos, G., Zhao, C., Yoon, K., Cook, J.M., Willert, K., Gaiano, N., and Reya, T. (2005). Integration of Notch and Wnt signaling in hematopoietic stem cell maintenance. Nat. Immunol. *6*, 314–322.

Elofsson, R., Andersson, A., Falck, B., and Sjöborg, S. (1984). The ciliated human keratinocyte. J. Ultrastruct. Res. *87*, 212–220.

Fan, S., Hurd, T.W., Liu, C.J., Straight, S.W., Weimbs, T., Hurd, E.A., Domino, S.E., and Margolis, B. (2004). Polarity proteins control ciliogenesis via kinesin motor interactions. Curr. Biol. *14*, 1451–1461.

Finetti, F., Paccani, S.R., Riparbelli, M.G., Giacomello, E., Perinetti, G., Pazour, G.J., Rosenbaum, J.L., and Baldari, C.T. (2009). Intraflagellar transport is required for polarized recycling of the TCR/CD3 complex to the immune synapse. Nat. Cell Biol. *11*, 1332–1339.

Fuchs, E. (2007). Scratching the surface of skin development. Nature *445*, 834–842.

Fuchs, E., Esteves, R.A., and Coulombe, P.A. (1992). Transgenic mice expressing a mutant keratin 10 gene reveal the likely genetic basis for epidermolytic hyperkeratosis. Proc. Natl. Acad. Sci. USA *15*, 6906–6910.

Gao, J., DeRouen, M.C., Chen, C.H., Nguyen, M., Nguyen, N.T., Ido, H., Harada, K., Sekiguchi, K., Morgan, B.A., Miner, J.H., et al. (2008). Laminin-511 is an epithelial message promoting dermal papilla development and function during early hair morphogenesis. Genes Dev. *22*, 2111–2124.

Gerdes, J.M., Davis, E.E., and Katsanis, N. (2009). The vertebrate primary cilium in development, homeostasis, and disease. Cell *137*, 32–45.

Goetz, S.C., and Anderson, K.V. (2010). The primary cilium: a signalling centre during vertebrate development. Nat. Rev. Genet. *11*, 331–344.

Gritli-Linde, A., Hallberg, K., Harfe, B.D., Reyahi, A., Kannius-Janson, M., Nilsson, J., Cobourne, M.T., Sharpe, P.T., McMahon, A.P., and Linde, A. (2007). Abnormal hair development and apparent follicular transformation to mammary gland in the absence of hedgehog signaling. Dev. Cell *12*, 99–112.

Han, Y.G., and Alvarez-Buylla, A. (2010). Role of primary cilia in brain development and cancer. Curr. Opin. Neurobiol. *20*, 58–67.

Haraguchi, K., Hayashi, T., Jimbo, T., Yamamoto, T., and Akiyama, T. (2006). Role of the kinesin-2 family protein, KIF3, during mitosis. J. Biol. Chem. *281*, 4094–4099.

Huangfu, D., Liu, A., Rakeman, A.S., Murcia, N.S., Niswander, L., and Anderson, K.V. (2003). Hedgehog signalling in the mouse requires intraflagellar transport proteins. Nature *426*, 83–87.

Jaulin, F., and Kreitzer, G. (2010). KIF17 stabilizes microtubules and contributes to epithelial morphogenesis by acting at MT plus ends with EB1 and APC. J. Cell Biol. *190*, 443–460.

Jonassen, J.A., San Agustin, J., Follit, J.A., and Pazour, G.J. (2008). Deletion of IFT20 in the mouse kidney causes misorientation of the mitotic spindle and cystic kidney disease. J. Cell Biol. *183*, 377–384.

Kennedy, J.R., Jr., and Brittingham, E. (1968). Fine structure changes during chloral hydrate deciliation of Paramecium caudatum. J. Ultrastruct. Res. *22*, 530–545.

Kopan, R., and Ilagan, M.X. (2009). The canonical Notch signaling pathway: unfolding the activation mechanism. Cell *137*, 216–233.

Lechler, T., and Fuchs, E. (2007). Desmoplakin: an unexpected regulator of microtubule organization in the epidermis. J. Cell Biol. *176*, 147–154.

Lehman, J.M., Laag, E., Michaud, E.J., and Yoder, B.K. (2009). An essential role for dermal primary cilia in hair follicle morphogenesis. J. Invest. Dermatol. *129*, 438–448.

Lin, F., Hiesberger, T., Cordes, K., Sinclair, A.M., Goldstein, L.S., Somlo, S., and Igarashi, P. (2003). Kidney-specific inactivation of the KIF3A subunit of kinesin-II inhibits renal ciliogenesis and produces polycystic kidney disease. Proc. Natl. Acad. Sci. USA *100*, 5286–5291.

Lowell, S., Jones, P., Le Roux, I., Dunne, J., and Watt, F.M. (2000). Stimulation of human epidermal differentiation by delta-notch signalling at the boundaries of stem-cell clusters. Curr. Biol. *10*, 491–500.

Luxenburg, C., Pasolli, H.A., Williams, S.E., and Fuchs, E. (2011). Developmental roles for Srf, cortical cytoskeleton and cell shape in epidermal spindle orientation. Nat. Cell Biol. *13*, 203–214.

Marszalek, J.R., Ruiz-Lozano, P., Roberts, E., Chien, K.R., and Goldstein, L.S. (1999). Situs inversus and embryonic ciliary morphogenesis defects in mouse mutants lacking the KIF3A subunit of kinesin-II. Proc. Natl. Acad. Sci. USA *96*, 5043–5048.

Mills, A.A., Zheng, B., Wang, X.J., Vogel, H., Roop, D.R., and Bradley, A. (1999). p63 is a p53 homologue required for limb and epidermal morphogenesis. Nature *398*, 708–713.

Mizutani, K., Yoon, K., Dang, L., Tokunaga, A., and Gaiano, N. (2007). Differential Notch signalling distinguishes neural stem cells from intermediate progenitors. Nature *449*, 351–355.

Morimoto, M., Liu, Z., Cheng, H.T., Winters, N., Bader, D., and Kopan, R. (2010). Canonical Notch signaling in the developing lung is required for determination of arterial smooth muscle cells and selection of Clara versus ciliated cell fate. J. Cell Sci. *123*, 213–224.

Moriyama, M., Durham, A.D., Moriyama, H., Hasegawa, K., Nishikawa, S., Radtke, F., and Osawa, M. (2008). Multiple roles of Notch signaling in the regulation of epidermal development. Dev. Cell *14*, 594–604.

Nigg, E.A., and Raff, J.W. (2009). Centrioles, centrosomes, and cilia in health and disease. Cell *139*, 663–678.

Nguyen, B.C., Lefort, K., Mandinova, A., Antonini, D., Devgan, V., Della Gatta, G., Koster, M.I., Zhang, Z., Wang, J., Tommasi di Vignano, A., et al. (2006). Cross-regulation between Notch and p63 in keratinocyte commitment to differentiation. Genes Dev. *20*, 1028–1042.

Okuyama, R., Nguyen, B.C., Talora, C., Ogawa, E., Tommasi di Vignano, A., Lioumi, M., Chiorino, G., Tagami, H., Woo, M., and Dotto, G.P. (2004). High commitment of embryonic keratinocytes to terminal differentiation through a Notch1-caspase 3 regulatory mechanism. Dev. Cell *6*, 551–562.

Oro, A.E., and Higgins, K. (2003). Hair cycle regulation of Hedgehog signal reception. Dev. Biol. *255*, 238–248.

Pan, J., and Snell, W. (2007). The primary cilium: keeper of the key to cell division. Cell *129*, 1255–1257.

Pedersen, L.B., and Rosenbaum, J.L. (2008). Intraflagellar transport (IFT) role in ciliary assembly, resorption and signalling. Curr. Top. Dev. Biol. *85*, 23–61.

Pugacheva, E.N., Jablonski, S.A., Hartman, T.R., Henske, E.P., and Golemis, E.A. (2007). HEF1-dependent Aurora A activation induces disassembly of the primary cilium. Cell *129*, 1351–1363.

Raghavan, S., Bauer, C., Mundschau, G., Li, Q., and Fuchs, E. (2000). Conditional ablation of beta1 integrin in skin. Severe defects in epidermal proliferation, basement membrane formation, and hair follicle invagination. J. Cell Biol. *150*, 1149–1160.

Santos, N., and Reiter, J.F. (2010). Tilting at nodal windmills: planar cell polarity positions cilia to tell left from right. Dev. Cell *19*, 5–6.

Satir, P., Pedersen, L.B., and Christensen, S.T. (2010). The primary cilium at a glance. J. Cell Sci. *123*, 499–503.

Schneider, L., Clement, C.A., Teilmann, S.C., Pazour, G.J., Hoffmann, E.K., Satir, P., and Christensen, S.T. (2005). PDGFRalphaalpha signaling is regulated through the primary cilium in fibroblasts. Curr. Biol. *15*, 1861–1866.

Schober, M., Raghavan, S., Nikolova, M., Polak, L., Pasolli, H.A., Beggs, H.E., Reichardt, L.F., and Fuchs, E. (2007). Focal adhesion kinase modulates tension signaling to control actin and focal adhesion dynamics. J. Cell Biol. *176*, 667–680.

Seeley, E.S., and Nachury, M.V. (2010). The perennial organelle: assembly and disassembly of the primary cilium. J. Cell Sci. *123*, 511–518.

Segre, J.A., Bauer, C., and Fuchs, E. (1999). Klf4 is a transcription factor required for establishing the barrier function of the skin. Nat. Genet. *22*, 356–360.

Soriano, P. (1999). Generalized lacZ expression with the ROSA26 Cre reporter strain. Nat. Genet. *21*, 70–71.

Taulman, P.D., Haycraft, C.J., Balkovetz, D.F., and Yoder, B.K. (2001). Polaris, a protein involved in left-right axis patterning, localizes to basal bodies and cilia. Mol. Biol. Cell *12*, 589–599.

Tien, A.C., Rajan, A., and Bellen, H.J. (2009). A Notch updated. J. Cell Biol. *184*, 621–629.

Vasioukhin, V., Bauer, C., Degenstein, L., Wise, B., and Fuchs, E. (2001). Hyperproliferation and defects in epithelial polarity upon conditional ablation of alpha-catenin in skin. Cell *104*, 605–617.

Vasioukhin, V., Degenstein, L., Wise, B., and Fuchs, E. (1999). The magical touch: genome targeting in epidermal stem cells induced by tamoxifen application to mouse skin. Proc. Natl. Acad. Sci. USA *96*, 8551–8556.

Wang, X., Pasolli, H.A., Williams, T., and Fuchs, E. (2008). AP-2 factors act in concert with Notch to orchestrate terminal differentiation in skin epidermis. J. Cell Biol. *183*, 37–48.

Williams, S.E., Beronja, S., Pasolli, H.A., and Fuchs, E. (2011). Asymmetric cell divisions promote Notch-dependent epidermal differentiation. Nature *470*, 353–358.

Wong, S.Y., Seol, A.D., So, P.L., Ermilov, A.N., Bichakjian, C.K., Epstein, E.H., Jr., Dlugosz, A.A., and Reiter, J.F. (2009). Primary cilia can both mediate and suppress Hedgehog pathway-dependent tumorigenesis. Nat. Med. *15*, 1055–1061.

Yamashita, Y.M., Mahowald, A.P., Perlin, J.R., and Fuller, M.T. (2007). Asymmetric inheritance of mother versus daughter centrosome in stem cell division. Science *315*, 518–521.

Yang, A., Schweitzer, R., Sun, D., Kaghad, M., Walker, N., Bronson, R.T., Tabin, C., Sharpe, A., Caput, D., Crum, C., and McKeon, F. (1999). p63 is essential for regenerative proliferation in limb, craniofacial and epithelial development. Nature *398*, 714–718.

Yi, R., O'Carroll, D., Pasolli, H.A., Zhang, Z., Dietrich, F.S., Tarakhovsky, A., and Fuchs, E. (2006). Morphogenesis in skin is governed by discrete sets of differentially expressed microRNAs. Nat. Genet. *38*, 356–362.